

Supporting Information

Phenylethynylantracene Based Push-Pull Molecular Systems: Tuning the Photophysics Through *Para*-substituent on the Phenyl Ring

Sonali Sahu, Parthasarathy Venkatakrishnan* and Ashok Kumar Mishra*
Department of Chemistry, Indian Institute of Technology Madras, Chennai 600036, Tamil Nadu, India

Experimental Details.

Synthetic Specifications. All the reagents were used as received without further purification. THF was dried and distilled over sodium-ketyl radical system. Triethylamine (TEA) and DMF were distilled using potassium hydroxide and calcium hydride, respectively. For reactions, clean oven-dried glasswares were used. The progress of the reactions was monitored by thin layer chromatography (TLC) using Merck silica-gel (60 F₂₅₄) precoated plates (0.25 mm) and the compound spot were seen with naked eye under a UV lamp (365 or 254 nm). The crude product obtained was then purified by column chromatography using silica gel (100-200 mesh). A mixture of hexane and chloroform was used as the eluent. Melting points of the compounds were measured by the open capillary method and the values were corrected. JASCO FT/IR-4100 spectrometer was used for recording the infrared spectra. ¹H (400 MHz) and ¹³C (100/125 MHz) NMR spectra were recorded using a Bruker Avance FT-NMR (400 and 500 MHz) spectrometer using CDCl₃ with TMS as the internal reference. The reported ¹H NMR and ¹³C spectra were calibrated with the residual proton solvent peak (CDCl₃, δ = 7.26 ppm) and residual carbon solvent peak (CDCl₃, δ = 77.16 ppm), respectively. High resolution Q-TOF mass spectrometer was used to obtain the High-resolution mass spectra.

Photophysical Studies. For this, all the solvents used were of spectroscopic grade. Stock solutions of 10⁻³ M for all compounds were prepared in DCM. Then the experimental samples were prepared by evaporating DCM from the required amount of stock solution by purging nitrogen gas and then adding the desired solvent in it. The molar extinction coefficients (ε) were calculated by taking three independent measurements at three different concentrations of the analyte with standard deviations ≤ 4 %.

Instrumentation. UV-visible absorption spectra were recorded with the help of a Shimadzu UV-2600 spectrophotometer using a quartz cuvette (path length 1 cm). The steady state fluorescence and anisotropy measurements were done using a Horiba Jobin-Yvon FluoroMax-4 fluorescence spectrophotometer with a 150 W xenon lamp as light source. To maintain the temperature of the fluorimeter cuvette holder, a CORIO CD-300F refrigerated/heating circulator from Julabo was used. Fluorescence lifetime measurements and anisotropy decay studies were carried out using a Horiba Jobin Yvon Fluorocube lifetime instrument with time-correlated single photon counting set up in reverse mode. The instrument response function (IRF) was collected using Ludox AS40 colloidal silica solution. The decays were analysed using IBH DAS6 software. A fit with $0.99 \leq \chi^2 \leq 1.30$ was considered as a good fit.

Quantum Yield Measurements. The fluorescence quantum yield (ϕ) of all the derivatives was measured using the following relation:

$$\phi_u = \phi_r \frac{F_u A_r \eta_u^2 q_r}{F_r A_u \eta_r^2 q_u} \quad (\text{S1})$$

where, ‘F’ represents the corrected fluorescence peak area, ‘A’ the absorbance at the excitation wavelength, ‘ η ’ the refractive index of the solvent used, ‘q’ the excitation light intensity, and the subscripts “r” and “u” refer to reference and unknown respectively. For calculating ϕ all the compounds in cyclohexane and MeCN, Coumarin 30 ($\phi = 0.67$ at 380 nm in MeCN) was used as a reference standard. For calculating ϕ of **AnPNO₂** in 1,4-dioxane and THF, Perylene ($\phi = 0.94$ at 410 nm in cyclohexane) was used as a reference standard. The radiative (k_r) and non-radiative (k_{nr}) rate constants were calculated using the formulae:

$$k_r = \frac{\phi}{\tau} \quad (\text{S2}) \quad \text{and} \quad k_{nr} = \frac{1}{\tau} - k_r \quad (\text{S3})$$

The ϕ values were calculated as the means of three independent measurements with standard deviations ≤ 3 %.

Theoretical Calculations. The computational calculations were performed using Gaussian 16 computational package. Optimization of ground state of the compounds was carried out using density functional theory (DFT) with B3LYP hybrid functional and 6-311+g(d,p) basis set without any symmetry constrains. Vibrational analyses were carried out to ascertain the absence of imaginary frequencies. The effect of solvent was included through self-consistent reaction field (SCRF) using polarizable continuum model (PCM). Excited state geometries were also optimized using B3LYP/6-311+g(d,p) combination. Potential energy surface (PES) scans were done using Relaxed redundant coordinate scan system using B3LYP/6-311+g(d,p). TD-DFT calculations for both absorption and emission were done using CAM-B3LYP functional and the same basis set. Electron density difference (EDD) between excited state and ground state [$\Delta\rho(r) = \rho^{S_1}(r) - \rho^{S_0}(r)$] were calculated using Multiwfn software where ρ^{S_1} and ρ^{S_0} must have the same geometry. $\Delta\rho$ can be divided into positive (ρ^+) and negative (ρ^-) parts, which indicate the regions where electron density has increased and decreased

respectively, after excitation. t -index is a measure of CT character in a molecule and is given by:¹

$$t \text{ index} = D \text{ index} - H_{CT} \quad (\text{S4})$$

Where D index (or d_{CT}) is the distance between the two barycenters of ρ^+ and ρ^- or the total CT length and H_{CT} is the average degree of spatial extension of ρ^+ and ρ^- in CT direction. If t -index is less than 0, it means that ρ^+ and ρ^- are not considerably separated due to CT. A positive value of t -index implies a significant separation of ρ^+ and ρ^- distributions due to CT and the transition should be identified as a typical CT transition.

Dipole Moment Change using Lippert-Mataga Equation. To understand the solvent polarity effect, the Lippert-Mataga equation² was used to correlate Stokes shift ($\Delta\bar{\nu}$) with orientation polarizability (Δf), which is given by:

$$\bar{\nu}_a - \bar{\nu}_f = \frac{2}{hc} \left(\frac{\epsilon - 1}{2\epsilon + 1} - \frac{n^2 - 1}{2n^2 + 1} \right) \frac{(\mu_E - \mu_G)^2}{a^3} + \text{constant} \quad (\text{S5})$$

Where $\bar{\nu}_a$ and $\bar{\nu}_f$ are the wavenumbers (cm^{-1}) corresponding to the absorption and the emission, respectively, h is the Planck's constant, c is the speed of light, and ' a ' is the radius of the solvent cavity in which the fluorophore resides. The equation involves both the dielectric constant (ϵ) and the refractive index (n) of the solvents. ' a ' was calculated as half of the length of the molecule in the optimised geometry using B3LYP/6-311+g(d,p).

Fluorescence Anisotropy Studies. Fluorescence anisotropy value (r) is given by the equation:³

$$r = \frac{I_{\parallel} - I_{\perp}}{I_{\parallel} + 2I_{\perp}} \quad (\text{S6})$$

Where I_{\parallel} and I_{\perp} are intensities of the emitted light parallel and perpendicular to the direction of the polarized excitation light, respectively. Time-resolved fluorescence anisotropy is given by:

$$r(t) = r_{\infty} + (r_0 - r_{\infty}) \exp(-t/\theta) \quad (\text{S7})$$

Where r_0 , r_{∞} and θ are the fundamental anisotropy, limiting/residual anisotropy and rotational correlation time. If the molecule is totally free to rotate, a r_{∞} value of zero is obtained. If there

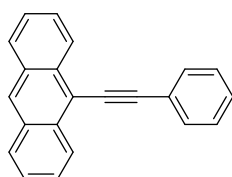
is hindered rotation i.e., the fluorophore is not fully free to rotate, a non-zero limiting anisotropy value is obtained.

Electrochemical Studies. Electrochemical measurements were done at room temperature (25 ± 1 °C) using the electrochemical workstation (CH Instruments 660A) at a scan rate of 0.1 V/s using three electrode system i.e., glassy carbon as working electrode, platinum wire as counter electrode and Ag/AgCl, KCl (saturated) as reference electrode. All the experiments were done in distilled and nitrogen-purged acetonitrile (MeCN) as the solvent using tetra-*n*-butylammonium hexafluorophosphate ($[n\text{-Bu}_4\text{N}][\text{PF}_6]$, 0.1 M) as the non-aqueous supporting electrolyte. All the cyclic voltammograms were calibrated using ferrocene (Fc) as the internal standard for each experiment and were corrected. The concentration of the analyte dyes was *ca.* 1 mM.

Preparation of WLE PVA Gel. The WLE solution in DMSO was prepared from **AnPCN** and **AnPNMe₂**. Then water was added to it so as to make the DMSO to water ratio 9:1 (v/v). After that, 12% (w/v) Polyvinyl alcohol (PVA) was added and the whole solution was stirred at 70 °C until all the PVA dissolved resulting in a transparent solution.⁴ Then it was immediately kept at 4 °C. The gel started forming after the solution cools down. The forming gel was kept at the same temperature (4 °C) for 2 days. Then it was used for experiments.

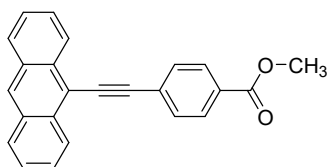
General procedure for Sonogashira Coupling: To an oven-dried two-neck round bottomed flask equipped with reflux condenser and a magnetic stir-bar, 9-bromoanthracene (1.0 equivalent) and a solvent mixture of THF and TEA (2:1, v/v) (or DMF and TEA mixture, 2:1, v/v) were added. The resulting solution was degassed with nitrogen gas for 5 minutes. Then the corresponding alkyne (1.0 equivalent), CuI (5 mol %) and the catalyst Pd(PPh₃)₂Cl₂ (4 mol % relative to the bromo derivative) were added carefully and the whole solution was again degassed with nitrogen gas for 15 minutes. Then the temperature was raised to 70 °C and stirring was continued for about 10-12 hours. The progress of the reaction was monitored using TLC. After the disappearance of the alkyne starting material, the reaction contents were cooled to room temperature, the solvents were evaporated, water was added and the organic contents were extracted with chloroform or ethyl acetate (3 times). The combined organic layer was washed with brine solution, dried over anhydrous sodium sulphate, filtered and the solvent was evaporated. The crude product was purified by silica-gel column chromatography using hexane and chloroform as the eluting solvents.

9-(Phenylethynyl)anthracene (AnP)



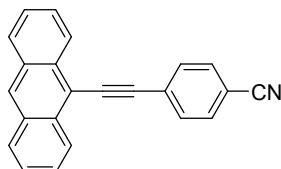
9-Bromoanthracene (0.35 g, 1.36 mmol) and ethynylbenzene (0.3 mL, 2.72 mmol) were Sonogashira-coupled in presence of Pd(PPh₃)₂Cl₂ (0.048 g, 0.068 mmol) and CuI (0.013 g, 0.068 mmol) in THF (4 mL) and TEA (2 mL) solvent mixture (2:1, v/v) at 70 °C. Time: 12 h. Yield: 0.358 g, 95%. Yellow Crystalline Solid. Mp: 106-108 °C. TLC: R_f = 0.55 in hexane. ¹H NMR (400 MHz, CDCl₃) δ: 8.66 (d, *J* = 8.8 Hz, 2H), 8.45 (s, 1H), 8.03 (d, *J* = 8.4 Hz, 2H), 7.78 (d, *J* = 6.8 Hz, 2H), 7.61 (t, *J* = 6.8 and 8.4 Hz, 2H), 7.52 (t, *J* = 7.6 Hz, 2H), 7.48-7.40 (m, 3H). ¹³C NMR (100 MHz, CDCl₃) δ: 132.8, 131.8, 131.3, 128.8, 128.7, 128.6, 127.9, 126.9, 126.7, 125.8, 123.8, 117.4, 100.9, 86.5. IR (KBr, cm⁻¹): 3052, 2955, 2922, 2852, 2197, 1656, 1623, 1582, 1462, 1084, 879, 849, 734. HR ESI-MS: [C₂₂H₁₄]⁺ = [M]⁺ calculated *m/z* = 278.1096; found *m/z* = 278.1086.

Methyl 4-(anthracen-9-ylethynyl)benzoate (AnPCO₂Me)



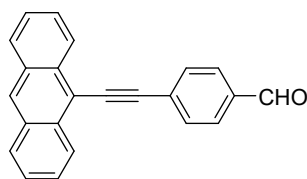
9-Bromoanthracene (0.35 g, 1.36 mmol) and methyl 4-ethynylbenzoate (0.24 g, 1.50 mmol) were Sonogashira-coupled in presence of Pd(PPh₃)₂Cl₂ (0.048 g, 0.068 mmol) and CuI (0.013 g, 0.068 mmol) in THF (4 mL) and TEA (2 mL) solvent mixture (2:1, v/v) at 70 °C. Time: 12 h. Yield: 0.421 g, 92%. Yellow Crystalline Solid. Mp: 178-180 °C. TLC: R_f = 0.31 (4:1, hexane/chloroform). ¹H NMR (400 MHz, CDCl₃) δ: 8.63 (d, *J* = 8.4 Hz, 2H), 8.47 (s, 1H), 8.12 (d, *J* = 8.4 Hz, 2H), 8.04 (d, *J* = 8.4 Hz, 2H), 7.83 (d, *J* = 8.0 Hz, 2H), 7.63 (t, *J* = 7.6 Hz, 2H), 7.53 (t, *J* = 8.0 and 7.2 Hz, 2H), 3.97 (s, 3H). ¹³C NMR (100 MHz, CDCl₃) δ: 166.7, 132.9, 131.6, 131.3, 129.8, 129.7, 128.9, 128.6, 128.4, 127.0, 126.7, 125.9, 116.7, 100.0, 89.5, 52.4. IR (KBr, cm⁻¹): 3018, 2956, 2917, 2848, 2195, 1720, 1703, 1655, 1638, 1461, 1332, 1282, 935, 763, 727, 690, 640, 621. HR ESI-MS: [C₂₄H₁₆O₂]⁺ = [M]⁺ calculated *m/z* = 336.1150; found *m/z* = 336.1156.

4-(Anthracen-9-ylethynyl)benzotrile (AnPCN)



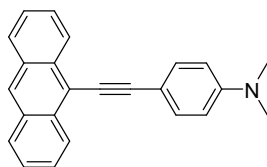
9-Bromoanthracene (0.1 g, 0.39 mmol) and 4-ethynylbenzotrile (0.059 g, 0.467 mmol) were Sonogashira-coupled in presence of Pd(PPh₃)₂Cl₂ (0.01 g, 0.014 mmol) and CuI (0.007 g, 0.037 mmol) in THF (2 mL) and TEA (1 mL) solvent mixture (2:1, v/v) at 70 °C. Time: 12 h. Yield: 0.058 g, 50%. Yellow Crystalline Solid. Mp: 170-172 °C. TLC: R_f = 0.28 (4:1, hexane/chloroform). ¹H NMR (400 MHz, CDCl₃) δ: 8.59 (d, *J* = 8.4 Hz, 2H), 8.51 (s, 1H), 8.05 (d, *J* = 8.4 Hz, 2H), 7.85 (d, *J* = 8.0 Hz, 2H), 7.74 (d, *J* = 8.0 Hz, 2H), 7.63 (t, *J* = 6.8 and 8.0 Hz, 2H), 7.55 (t, *J* = 7.6 Hz, 2H). ¹³C NMR (125 MHz, CDCl₃) δ: 133.0, 132.4, 132.2, 131.3, 129.1, 129.0, 128.6, 127.3, 126.5, 126.0, 118.8, 116.1, 111.7, 99.0, 91.0. IR (KBr, cm⁻¹): 2957, 2918, 2850, 2228, 2195, 1738, 1721, 1674, 1582, 1463, 1283, 1260, 1092, 1027, 802, 758, 691. HR ESI-MS: [C₂₃H₁₃N]⁺ = [M]⁺ calculated *m/z* = 303.1048; found *m/z* = 303.1029.

4-(Anthracen-9-ylethynyl)benzaldehyde (AnPCHO)



9-Bromoanthracene (0.35 g, 1.36 mmol) and 4-ethynylbenzaldehyde (0.23 g, 1.77 mmol) were Sonogashira-coupled in presence of Pd(PPh₃)₂Cl₂ (0.048 g, 0.068 mmol) and CuI (0.013 g, 0.068 mmol) in THF (4 mL) and TEA (2 mL) solvent mixture (2:1, v/v) at 70 °C. Time: 11 h. Yield: 0.312 g, 75%. Yellow Crystalline Solid. Mp: 140-142 °C. TLC: R_f = 0.23 (4:1, hexane/chloroform). ¹H NMR (400 MHz, CDCl₃) δ: 10.08 (s, 1H), 8.63 (d, *J* = 8.4 Hz, 2H), 8.50 (s, 1H), 8.05 (d, *J* = 8.4 Hz, 2H), 7.97 (d, *J* = 8.4 Hz, 2H), 7.92 (d, *J* = 8.0 Hz, 2H), 7.64 (t, *J* = 6.8 and 8.0 Hz, 2H), 7.54 (t, *J* = 8.0 and 7.2 Hz, 2H). ¹³C NMR (125 MHz, CDCl₃) δ: 191.6, 135.6, 132.9, 132.2, 131.3, 130.0, 129.9, 129.0, 128.9, 127.2, 126.6, 125.9, 116.4, 100.0, 90.7. IR (KBr, cm⁻¹): 3053, 2955, 2922, 2850, 2730, 2192, 1699, 1658, 1598, 1562, 1206, 1164, 886, 835, 737. HR ESI-MS: [C₂₃H₁₄O]⁺ = [M]⁺ calculated *m/z* = 306.1045; found *m/z* = 306.1063.

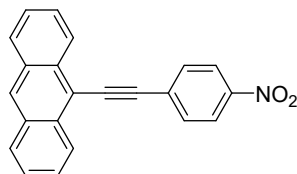
4-(Anthracen-9-ylethynyl)-N,N-dimethylaniline (AnPNMe₂)



9-Bromoanthracene (0.2 g, 0.78 mmol) and 4-ethynyl-*N,N*-dimethylaniline (0.102 g, 0.702 mmol) were Sonogashira-coupled in presence of Pd(PPh₃)₂Cl₂ (0.022 g, 0.031 mmol) and CuI (0.007 g, 0.037 mmol) in DMF (1.5 mL) and TEA (1.5 mL) solvent mixture (1:1, v/v) at 70 °C. Time: 10 h. Yield: 0.175 g, 70%. Yellow Crystalline Solid. Mp: 193-195 °C. TLC: R_f = 0.34 (4:1, hexane/chloroform). ¹H NMR (400 MHz, CDCl₃) δ: 8.69 (d, *J* = 8.8 Hz, 2H), 8.38 (s, 1H), 8.01 (d, *J* = 8.4 Hz, 2H), 7.65 (d, *J* = 8.8 Hz, 2H), 7.58 (t, *J* = 6.8 and 8.0 Hz, 2H), 7.50 (t, *J* = 7.6 and 7.2 Hz, 2H), 6.76 (d, *J* = 8.8 Hz, 2H), 3.04 (s, 6H). ¹³C NMR (125 MHz, CDCl₃) δ: 150.6, 133.0, 132.5, 131.5, 128.7, 127.3, 126.7, 126.3, 125.7, 118.7, 112.2, 110.7, 102.5, 84.6, 40.4. IR (KBr, cm⁻¹): 3049, 2956, 2918, 2851, 2181, 1656, 1605, 1524, 1461, 1440, 1376,

1360, 1230, 1188, 1064, 1038, 1015, 876, 814, 735. HR ESI-MS: $[C_{24}H_{19}N]^+ = [M]^+$ calculated $m/z = 321.1517$; found $m/z = 321.1506$.

9-((4-Nitrophenyl)ethynyl)anthracene (AnPNO₂)



9-Bromoanthracene (0.5 g, 1.9 mmol) and 1-ethynyl-4-nitrobenzene (0.364 g, 2.47 mmol) were Sonogashira-coupled in presence of $Pd(PPh_3)_2Cl_2$ (0.054 g, 0.076 mmol) and CuI (0.036 g, 0.19 mmol) in THF (8 mL) and TEA (4 mL) solvent mixture (2:1, v/v) at 70 °C. Time: 12 h. Yield: 0.32 g, 51%. Yellow Crystalline Solid. Mp: 208-210 °C. TLC: $R_f = 0.50$ (4:1, hexane/chloroform). 1H NMR (400 MHz, $CDCl_3$) δ : 8.60 (d, $J = 8.8$ Hz, 2H), 8.52 (s, 1H), 8.32 (d, $J = 8.8$ Hz, 2H), 8.06 (d, $J = 8.4$ Hz, 2H), 7.90 (d, $J = 8.8$ Hz, 2H), 7.67-7.63 (m, 2H), 7.57-7.52 (m, 2H). ^{13}C NMR (125 MHz, $CDCl_3$) δ : 147.1, 133.0, 132.3, 131.3, 130.6, 129.3, 129.1, 127.3, 126.5, 126.0, 123.9, 115.9, 98.9, 91.9. IR (KBr, cm^{-1}): 2959, 2920, 2850, 2197, 1658, 1589, 1512, 1339, 1259, 1101, 1026, 893, 848, 799, 741, 615. HR ESI-MS: $[C_{22}H_{13}NO_2 + NH_4]^+ = [M + NH_4]^+$ calculated $m/z = 341.1290$; found $m/z = 341.1281$.

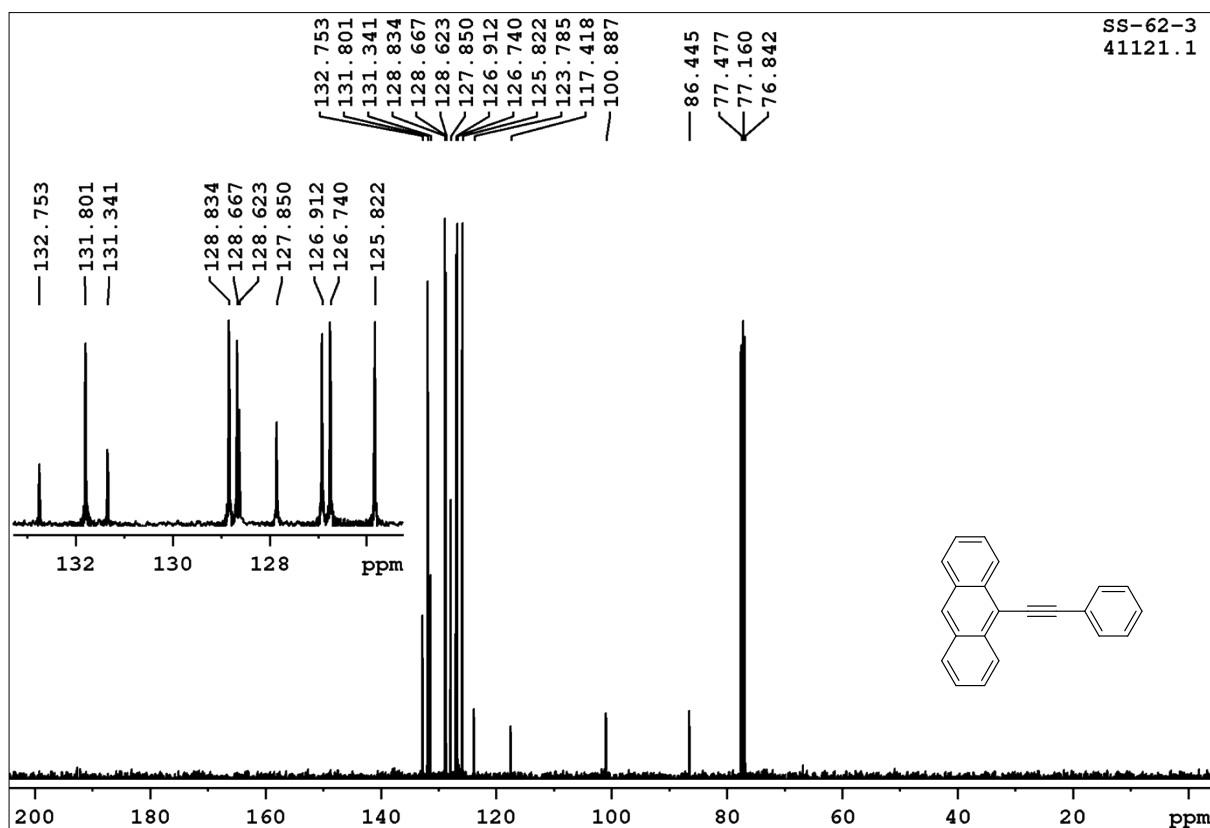
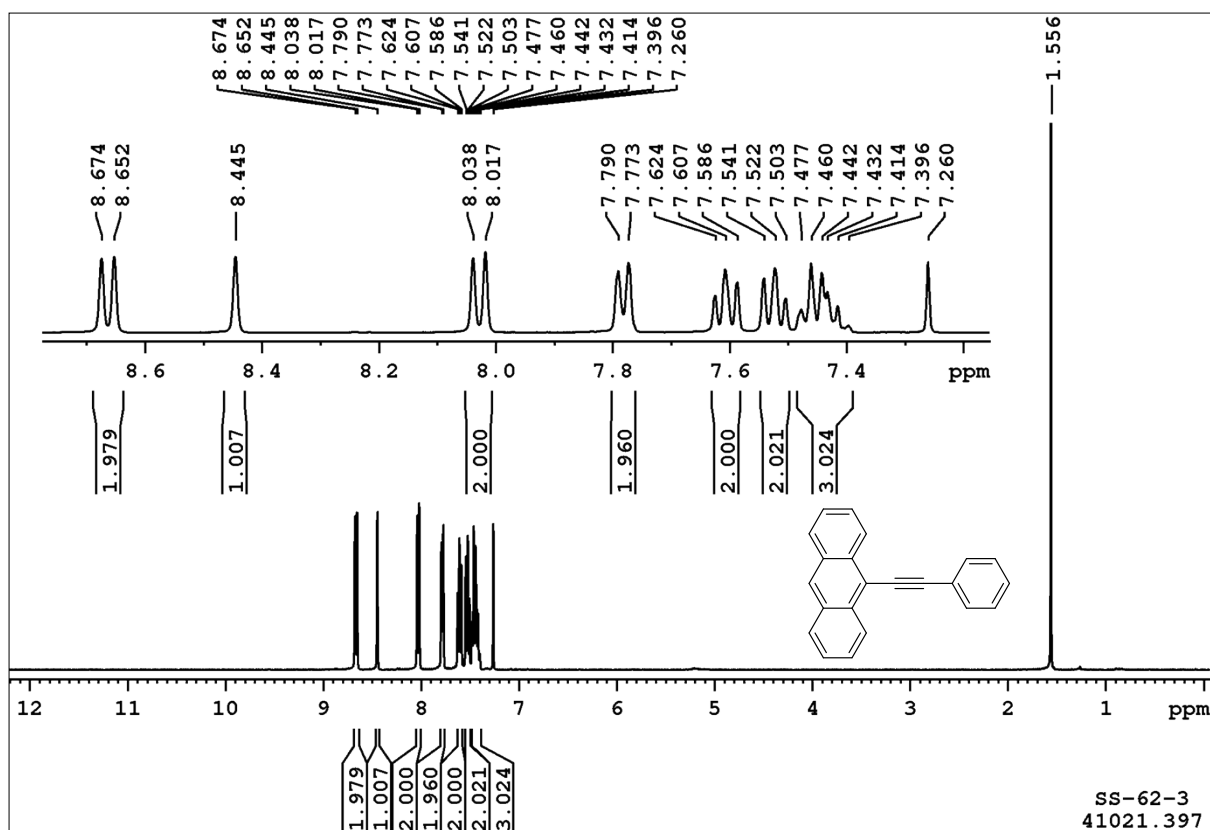


Fig. S1. ¹H NMR (top) and ¹³C NMR (bottom) spectra of AnP in CDCl₃.

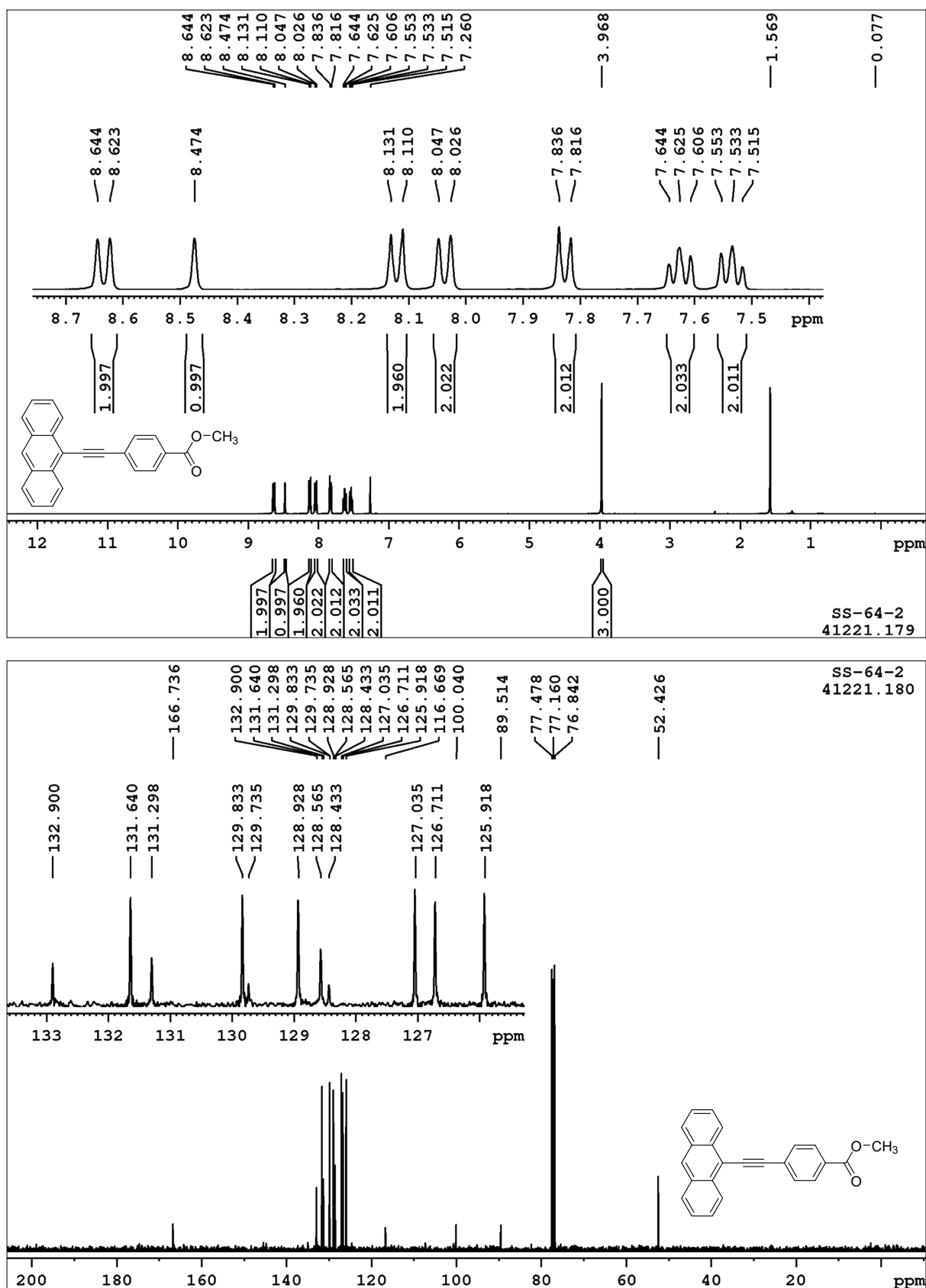


Fig. S2. ¹H NMR (top) and ¹³C NMR (bottom) spectra of AnPCO₂Me in CDCl₃.

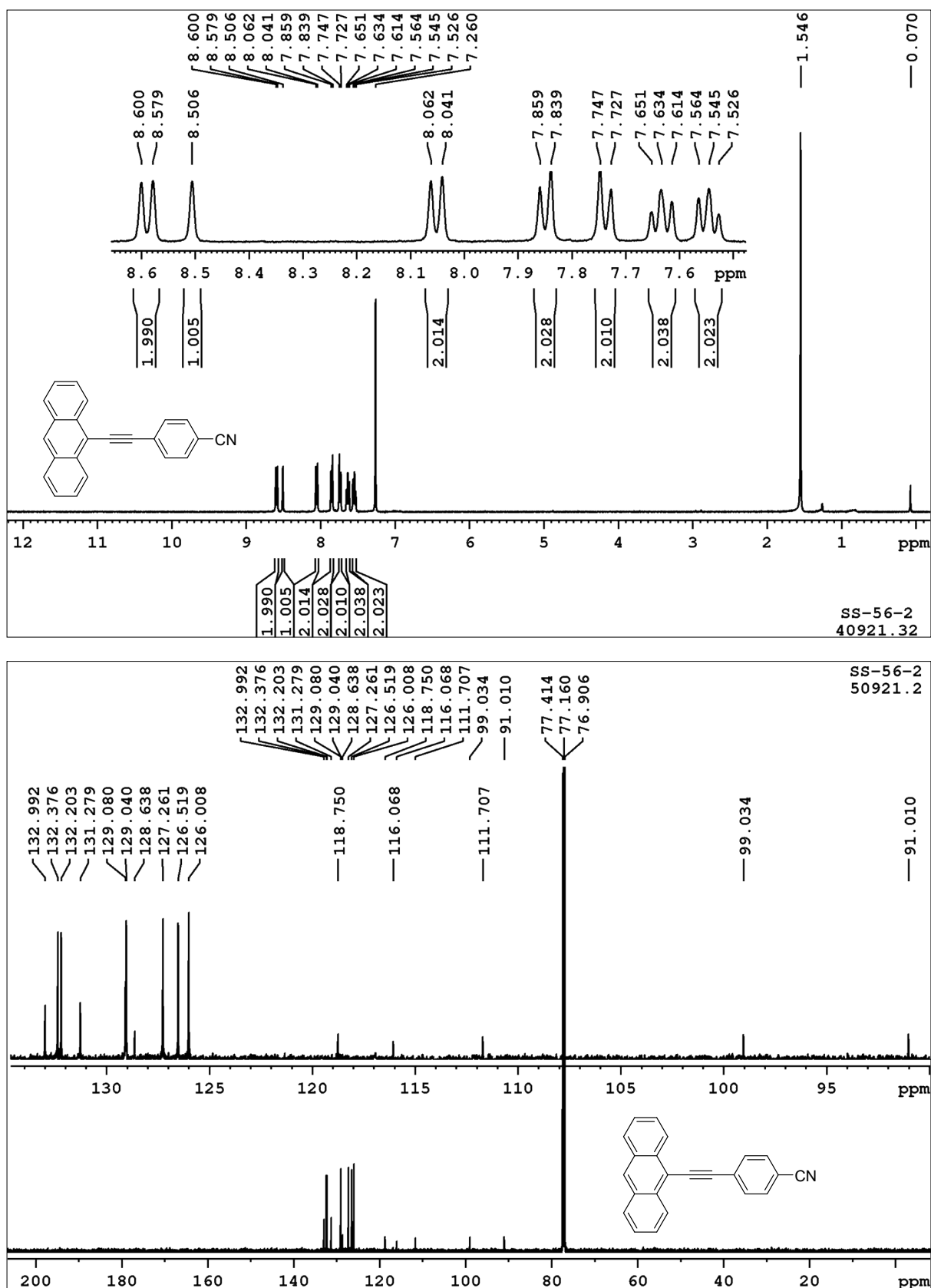


Fig. S3. ¹H NMR (top) and ¹³C NMR (bottom) spectra of AnPCN in CDCl₃.

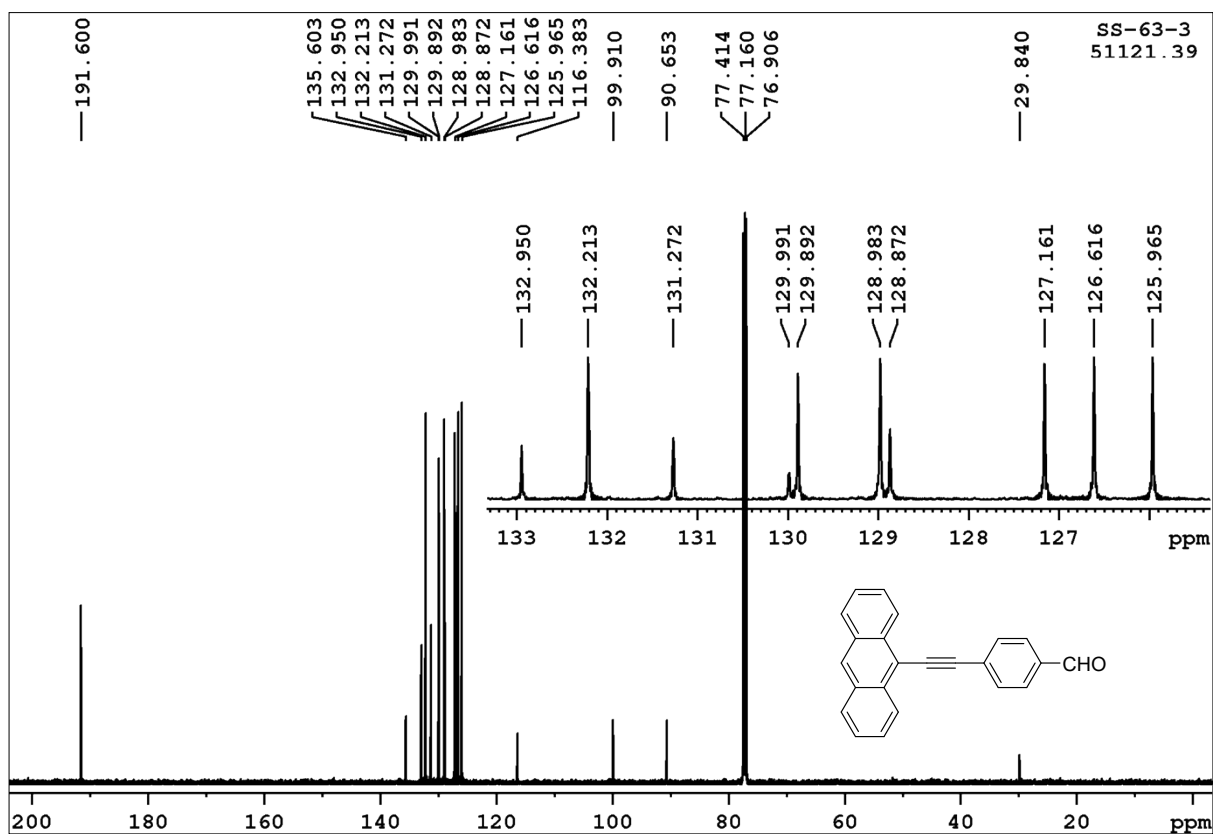
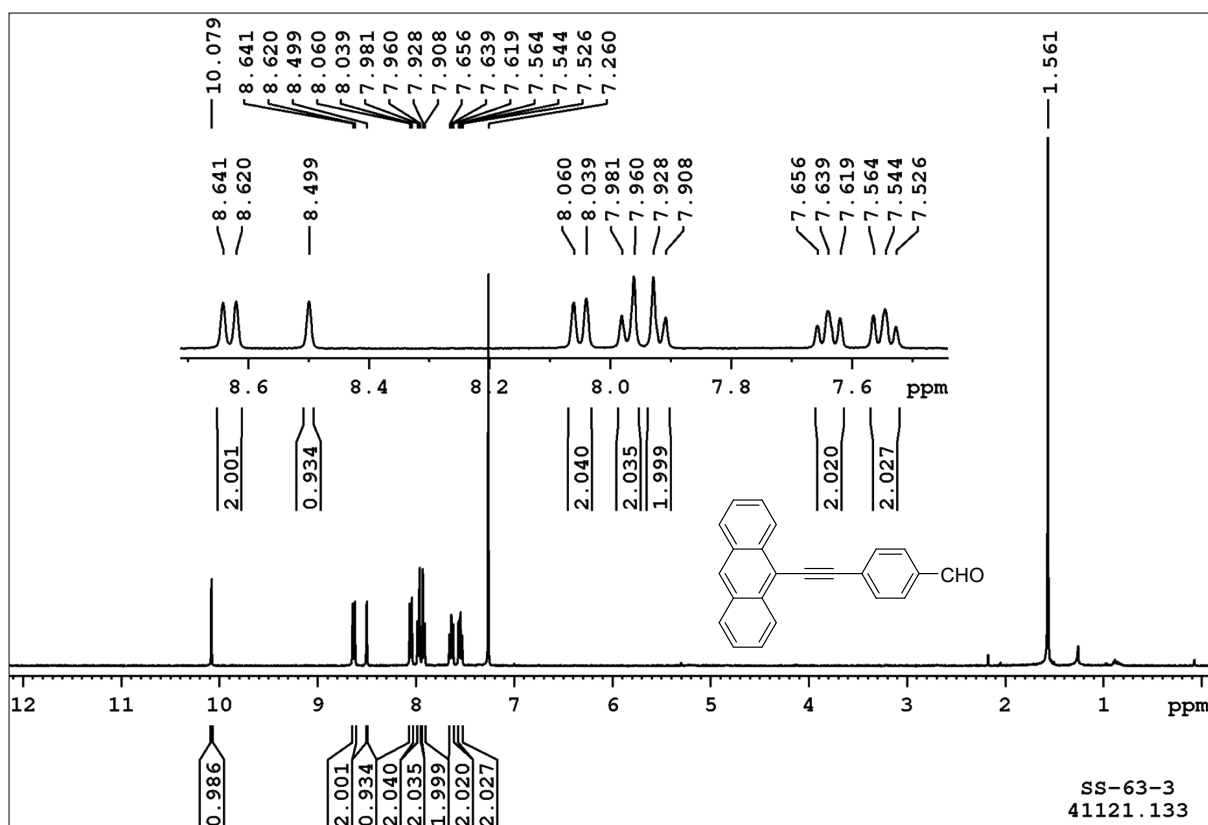


Fig. S4. ¹H NMR (top) and ¹³C NMR (bottom) spectra of AnPCHO in CDCl₃.

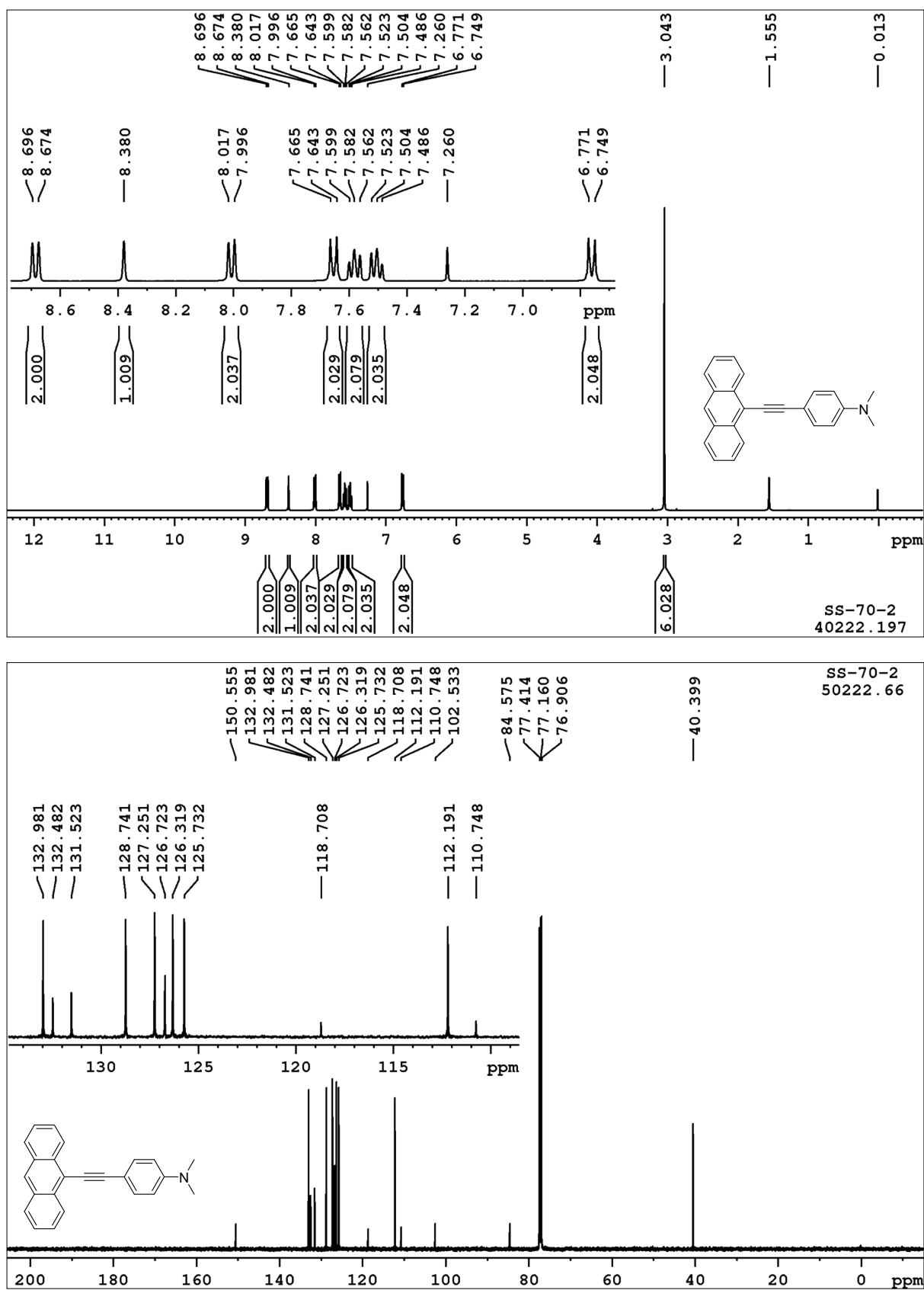


Fig. S5. ¹H NMR (top) and ¹³C NMR (bottom) spectra of AnPNMe₂ in CDCl₃.

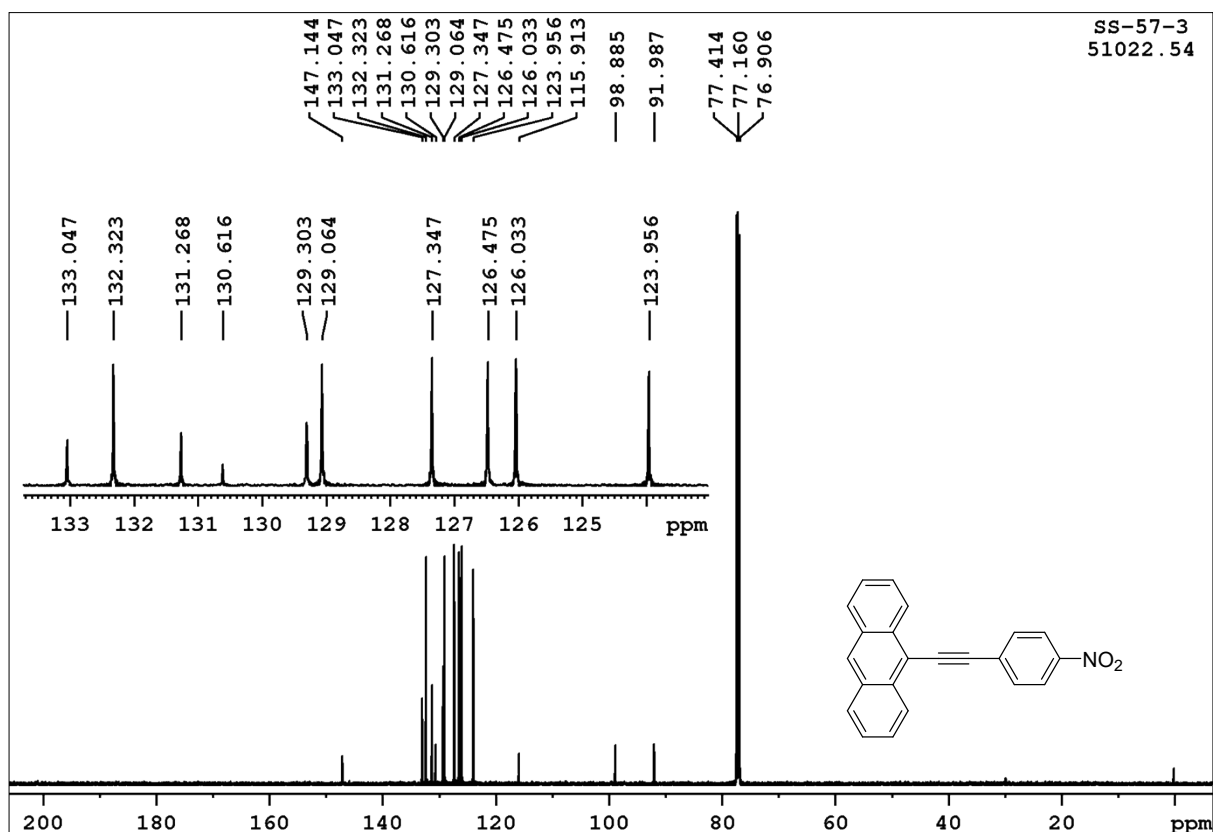
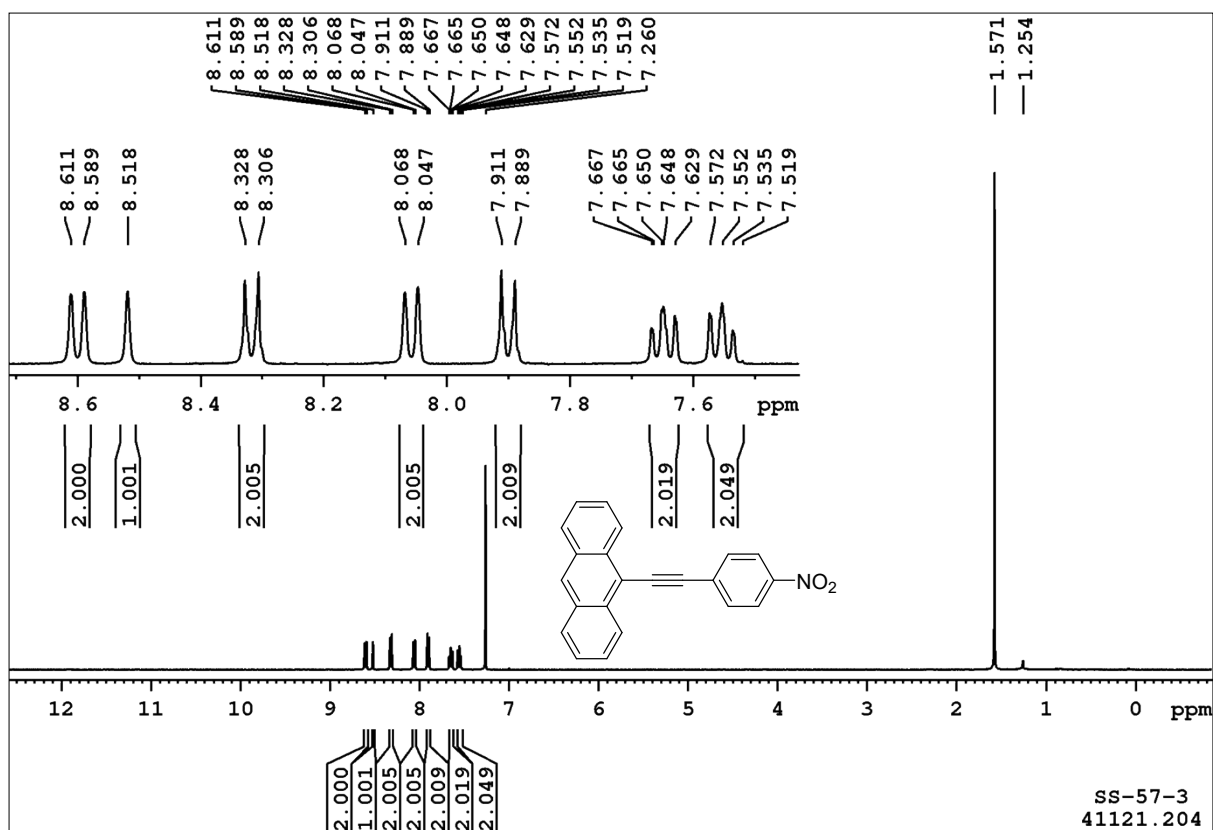


Fig. S6. ¹H NMR (top) and ¹³C NMR (bottom) spectrum of AnPNO₂ in CDCl₃.

Table S1. Absorption, emission parameters and Stokes shifts of **AnP**, **AnPCO₂Me** and **AnPCN** in solvents of varying polarities.

Solvents	AnP			AnPCO₂Me			AnPCN		
	λ_{abs} (nm)	λ_{em} (nm)	Stokes shift (cm ⁻¹)	λ_{abs} (nm)	λ_{em} (nm)	Stokes shift (cm ⁻¹)	λ_{abs} (nm)	λ_{em} (nm)	Stokes shift (cm ⁻¹)
n-Heptane	374, 393, 415	422, 448, 473	400	382, 401, 423	429, 455, 483	331	384, 402, 426	430, 457, 484	218
Cyclohexane	375, 394, 416	423, 449, 476	398	383, 402, 424	430, 457, 485	329	385, 404, 427	432, 459, 487	271
1,4-Dioxane	377, 397, 419	428, 454, 480	502	385, 405, 427	437, 463, 491	536	387, 406, 428	440, 465, 494(sh)	637
THF	378, 397, 419	428, 454, 480	502	386, 405, 427	439, 464, 494	640	387, 406, 428	443, 467, 494(sh)	791
DCM	380, 398, 420	429, 456, 484	500	385, 405, 428	440, 465, 494	637	387, 407, 430	444, 468, 498(sh)	733
Methanol	375, 393, 415	425, 450, 477	567	383, 401, 423	439, 460	862	385, 402, 425	444, 463	1007
Ethanol	375, 394, 416	425, 451, 477	509	384, 402, 424	439, 461	806	386, 404, 426	443, 465	901
2-Propanol	375, 394, 415	425, 451, 477	567	384, 402, 424	439, 461	806	386, 404, 426	443, 466	901
MeCN	375, 395, 417	427, 453, 479	562	384, 402, 424	440, 461	858	387, 403, 426	445, 464	1002
DMF	380, 399, 421	431, 458, 485	551	386, 406, 429	446, 468	888	387, 408, 430	451, 470	1083

Table S2. Absorption, emission parameters and Stokes shifts of **AnPCHO**, **AnPNMe₂** and **AnPNO₂** in solvents of varying polarities.

Solvents	AnPCHO			AnPNMe₂			AnPNO₂		
	λ_{abs} (nm)	λ_{em} (nm)	Stokes shift (cm ⁻¹)	λ_{abs} (nm)	λ_{em} (nm)	Stokes shift (cm ⁻¹)	λ_{abs} (nm)	λ_{em} (nm)	Stokes shift (cm ⁻¹)
n-Heptane	385, 405, 429	434, 461, 491	269	385, 411, 436	450, 477, 508	714	394, 414, 439	446, 474, 503	358
Cyclohexane	386, 407, 430	436, 463, 492	320	386, 413, 437	452, 479, 510	759	397, 416, 442	449, 477, 506	353
1,4-Dioxane	388, 408, 431	447, 471	830	390, 418, 439	493	2495	390, 417, 438	520	3600
THF	388, 409, 432	471	1917	391, 419, 439	530	3911	390, 417, 437	551	4734
DCM	390, 410, 434	479	2165	392, 420, 440	524	3643	392, 420, 438	617	6624
Methanol	385, 405, 425	425, 450, 478	0	385, 413, 431	548	4954	388, 412, 432	522	3991
Ethanol	387, 406, 428	425, 451, 478	-	387, 416, 434	535	4350	388, 414, 434	516	3662
2-Propanol	386, 407, 429	426, 453, 520	4079	388, 416, 432	527	4173	387, 414, 434	506	3279
MeCN	387, 406, 428	499	3324	387, 416, 435	569	5414	388, 413, 432	639	7499
DMF	390, 410, 433	495	2893	393, 421, 441	574	5254	392, 418, 437	628	6960

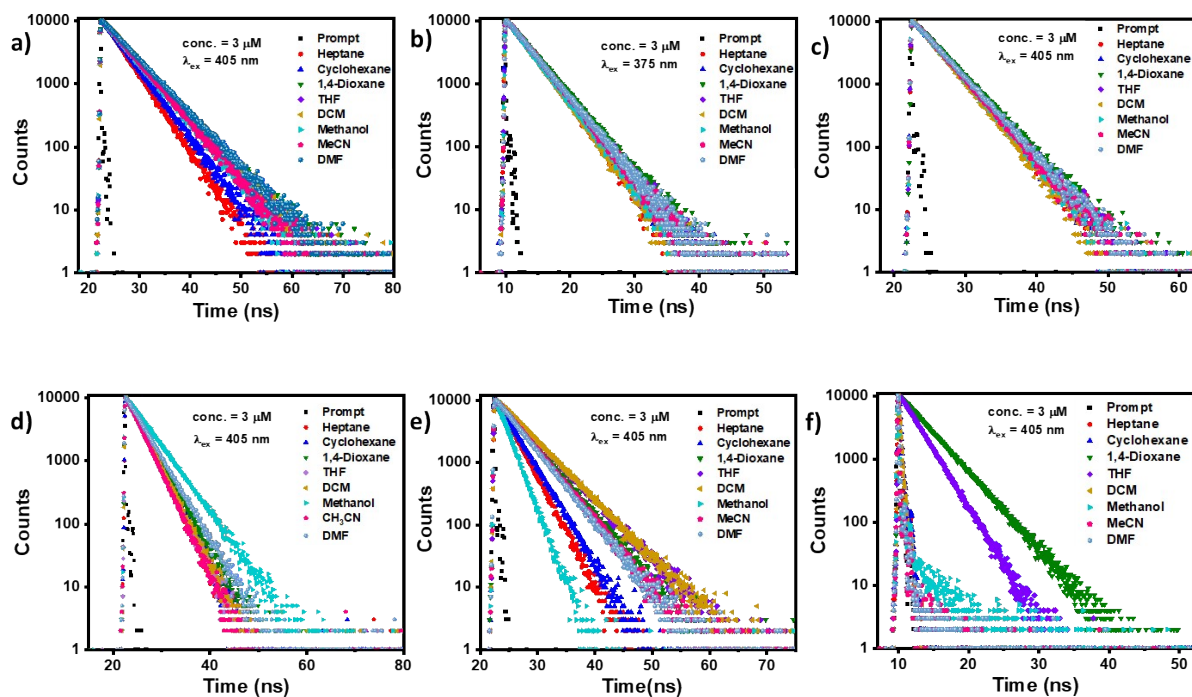


Fig. S7. Fluorescence decay profiles of (a) AnP, (b) AnPCO₂Me ($\lambda_{\text{ex}} = 375$ nm), (c) AnPCN, (d) AnPCHO, (e) AnPNMe₂ and (f) AnPNO₂ ($\lambda_{\text{ex}} = 405$ nm) (3×10^{-6} M) in solvents of different polarities.

Table S3. Fluorescence decay data of AnP, AnPCO₂Me and AnPCN in solvents of varying polarities. (β is the contribution of each emitting species towards the total emission and α is the population of the emitting species.)

Solvents	AnP ($\lambda_{\text{ex}} = 405$ nm)			AnPCO ₂ Me ($\lambda_{\text{ex}} = 375$ nm)			AnPCN ($\lambda_{\text{ex}} = 405$ nm)		
	λ_{em}	$\tau(\text{ns})(\beta)(\alpha)$	χ^2	λ_{em}	$\tau(\text{ns})(\beta)(\alpha)$	χ^2	λ_{em}	$\tau(\text{ns})(\beta)(\alpha)$	χ^2
Heptane	422	3.58(100)(100)	1.17	429	3.16(100)(100)	1.13	430	3.24(100)(100)	1.08
Cyclohexane	423	4.00(100)(100)	1.05	430	3.29(100)(100)	1.12	432	3.32(100)(100)	1.15
1,4-Dioxane	428	4.91(100)(100)	1.10	437	3.58(100)(100)	1.14	440	3.59(100)(100)	1.26
THF	427	4.70(100)(100)	1.17	439	3.35(100)(100)	1.20	443	3.40(100)(100)	1.16
DCM	430	4.93(100)(100)	1.12	440	3.12(100)(100)	1.15	444	3.13(100)(100)	1.12
Methanol	425	4.56(100)(100)	1.15	439	3.25(100)(100)	1.04	444	3.32(100)(100)	1.00
MeCN	427	4.64(100)(100)	1.03	440	3.36(100)(100)	1.12	445	3.34(100)(100)	1.00
DMF	431	5.08(100)(100)	1.13	446	3.42(100)(100)	1.19	452	3.49(100)(100)	1.17

Table S4. Fluorescence decay data of **AnPCHO**, **AnPNMe₂** and **AnPNO₂** in solvents of varying polarities.

Solvents	AnPCHO ($\lambda_{ex} = 405$ nm)			AnPNMe₂ ($\lambda_{ex} = 405$ nm)			AnPNO₂ ($\lambda_{ex} = 405$ nm)		
	λ_{em}	$\tau(ns)(\beta)(\alpha)$	χ^2	λ_{em}	$\tau(ns)(\beta)(\alpha)$	χ^2	λ_{em}	$\tau(ns)(\beta)(\alpha)$	χ^2
Heptane	434	2.71(100)(100)	1.20	451	2.49(100)(100)	1.18	446	0.1(100)(100)	1.29
Cyclohexane	436	2.81(100)(100)	1.20	452	2.84(100)(100)	1.06	449	0.2(100)(100)	1.27
1,4-Dioxane	447	3.08(100)(100)	1.20	499	4.01(100)(100)	1.09	520	3.78(100)(100)	1.10
THF	471	2.71(100)(100)	1.23	530	3.98(100)(100)	1.12	551	2.37(100)(100)	1.22
DCM	479	2.77(100)(100)	1.20	524	4.62(100)(100)	1.02	617	-	-
Methanol	424	4.08(100)(100)	1.20	548	1.79(100)(100)	1.19	522	-	-
MeCN	499	2.63(100)(100)	1.17	569	3.86(100)(100)	1.01	639	-	-
DMF	495	3.32(100)(100)	1.20	575	3.75(100)(100)	1.00	628	-	-

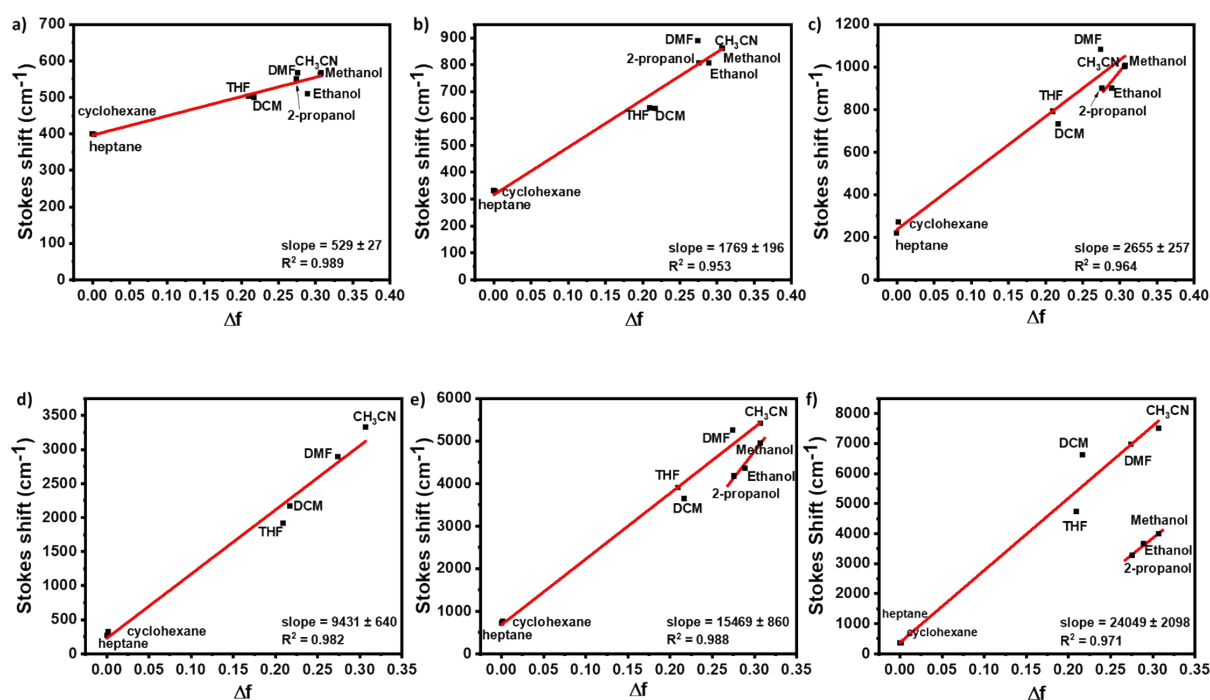


Fig. S8. Lippert-Mataga plots for (a) **AnP**, (b) **AnPCO₂Me**, (c) **AnPCN**, (d) **AnPCHO**, (e) **AnPNMe₂** and (f) **AnPNO₂**.

Table S5. t -indices, q_{CT} , d_{CT} and ICT operative change in dipole moment ($\mu_e - \mu_g$) of the compounds calculated from electron density difference plots.

Compound	AnP	AnPCO ₂ Me	AnPCN	AnPCHO	AnPNMe ₂	AnPNO ₂
t -index (Å)	-1.933	-0.555	-0.163	0.766	0.975	1.962
q_{CT} (a.u.)	0.301	0.423	0.441	0.547	0.615	0.815
d_{CT} (Å°)	0.480	2.811	3.112	4.226	4.498	5.558
$\Delta\mu$ (D)	0.72	5.90	6.64	11.09	13.28	21.76

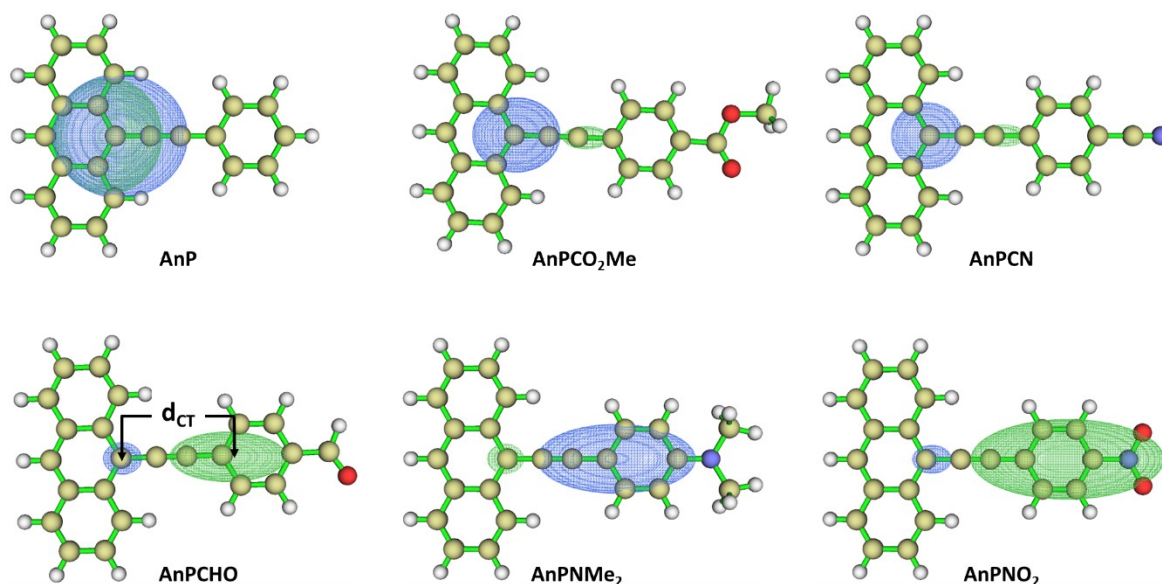
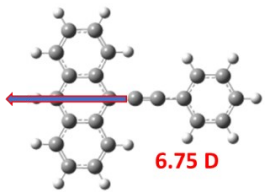
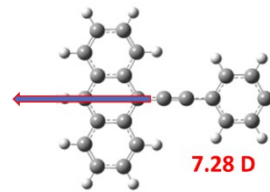
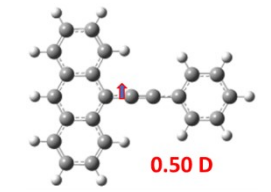
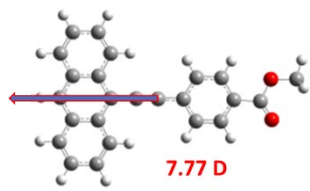
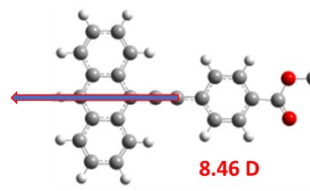
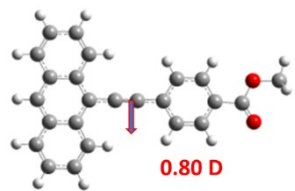
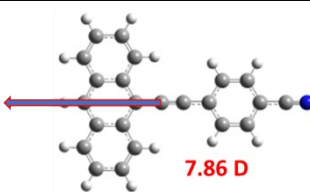
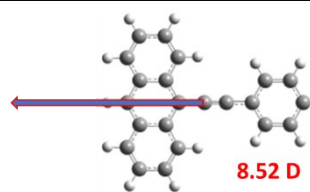
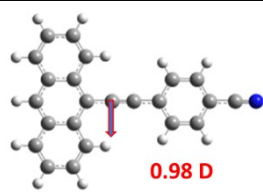
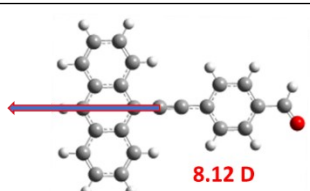
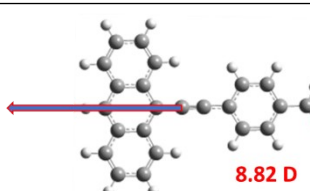
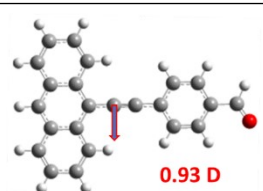
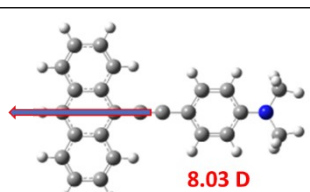
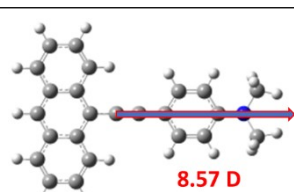
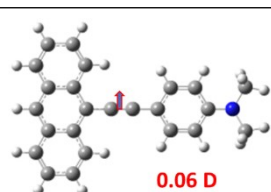
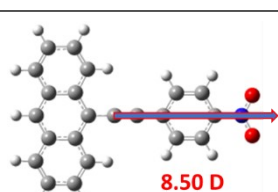
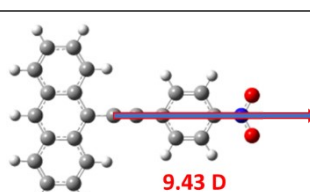
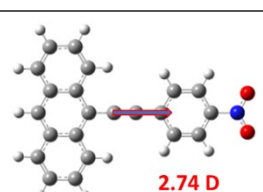


Fig. S9. Plots of positive and negative parts of $\Delta\rho(r)$. Green and blue regions indicate the positive (ρ^+) and negative (ρ^-) parts of $\Delta\rho$ respectively. Different iso-surface values are adjusted so as just to visualize both the regions.

Table S6. Calculated transition dipole moment vectors of the compounds (arrows show their directions and magnitudes are in red fonts) for $S_0 \rightarrow S_1$ (absorption), $S_1 \rightarrow S_0$ (emission) and $S_0 \rightarrow S_2$ (absorption) in cyclohexane using CAM-B3LYP/6-311+g(d,p) level of theory.

Compound	Directions of Transition Dipole Moment Vectors and their Magnitudes in debye		
	$S_0 \rightarrow S_1$	$S_1 \rightarrow S_0$	$S_0 \rightarrow S_2$
AnP	 6.75 D	 7.28 D	 0.50 D
AnPCO ₂ Me	 7.77 D	 8.46 D	 0.80 D
AnPCN	 7.86 D	 8.52 D	 0.98 D
AnPCHO	 8.12 D	 8.82 D	 0.93 D
AnPNMe ₂	 8.03 D	 8.57 D	 0.06 D
AnPNO ₂	 8.50 D	 9.43 D	 2.74 D

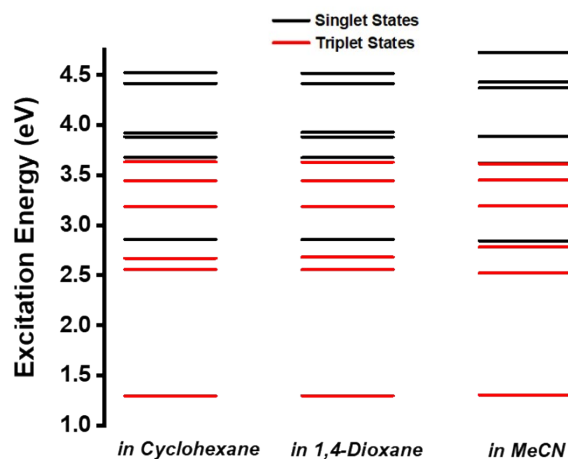


Fig. S10. Vertical excitation energies for singlet (black lines) and triplet (red lines) states of AnPNO₂ in cyclohexane, 1,4-dioxane and MeCN using CAM-B3LYP/6-311+g(d,p).

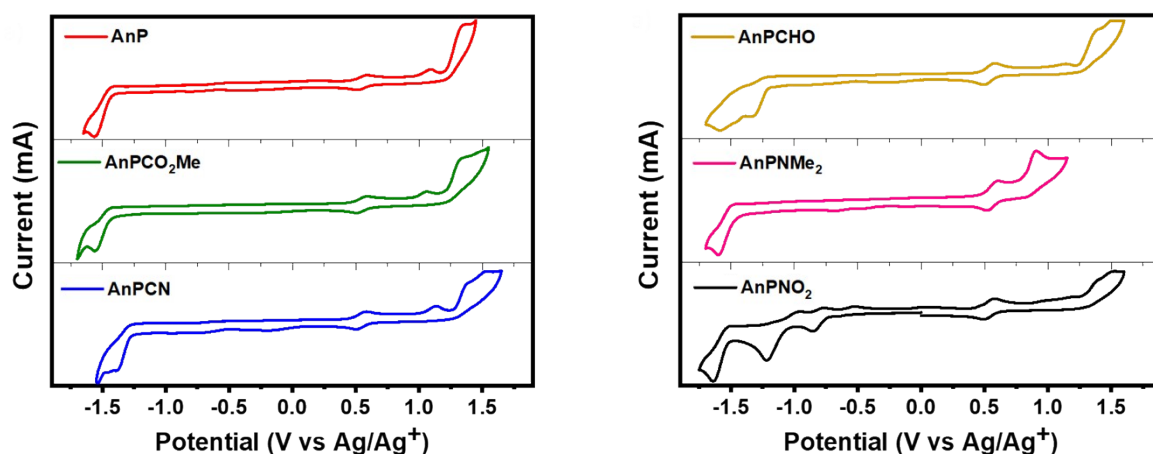


Fig. S11. Cyclic voltammograms of the compounds with Fc/Fc⁺ in MeCN.

Table S7. Electrochemical properties of the compounds recorded in MeCN.

Compound	$E_{\text{onset}}(\text{ox})$ (V)	$E_{\text{onset}}(\text{red})$ (V)	$E_{\text{HOMO}}^{\text{a}}$ (eV)	$E_{\text{LUMO}}^{\text{b}}$ (eV)	$E_{\text{g}}^{\text{CV c}}/E_{\text{g}}^{\text{opt d}}$ (eV)
AnP	+0.97	-1.42	-5.31	-2.76	2.55/2.88
AnPCO ₂ Me	+0.96	-1.44	-5.30	-2.74	2.56/2.81
AnPCN	+1.02	-1.29	-5.36	-2.90	2.46/2.79
AnPCHO	+0.90	-1.22	-5.24	-2.97	2.27/2.76
AnPNMe ₂	+0.80	-1.47	-5.12	-2.71	2.41/2.64
AnPNO ₂	+0.89	-0.75	-5.23	-3.45	1.78/2.58

The first oxidation and reduction of the cyclic voltammograms were considered for the calculations. E_{g} is the energy gap between HOMO and LUMO and λ_{onset} is the onset of the UV-visible absorption spectra (here taken in MeCN).

$$^{\text{a}}E_{\text{HOMO}} = -[E_{\text{onset}}(\text{oxidation}) + 4.8 - E_{\text{FC}}] \text{ eV}; \quad ^{\text{b}}E_{\text{LUMO}} = -[E_{\text{onset}}(\text{reduction}) + 4.8 - E_{\text{FC}}] \text{ eV}; \quad ^{\text{c}}E_{\text{g}}^{\text{CV}} = E_{\text{LUMO}} - E_{\text{HOMO}}; \quad ^{\text{d}}E_{\text{g}}^{\text{opt}} = (1240/\lambda_{\text{onset}}) \text{ eV}$$

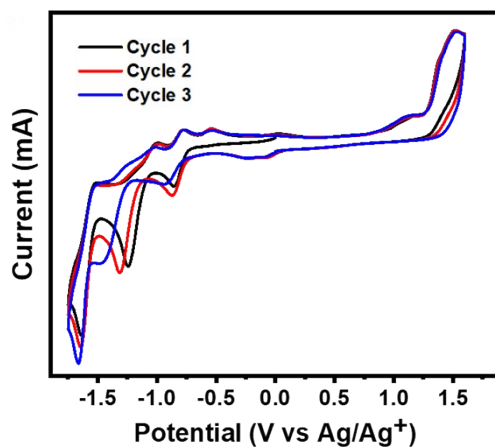


Fig. S12. Cyclic voltammogram of AnPNO_2 for three consecutive cycles in MeCN showing its electrochemical instability.

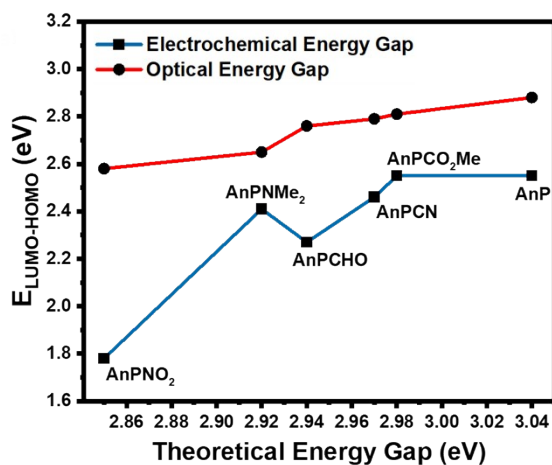


Fig. S13. Comparison of optical and electrochemical energy gap (HOMO-LUMO gap) with respect to the theoretical ones.

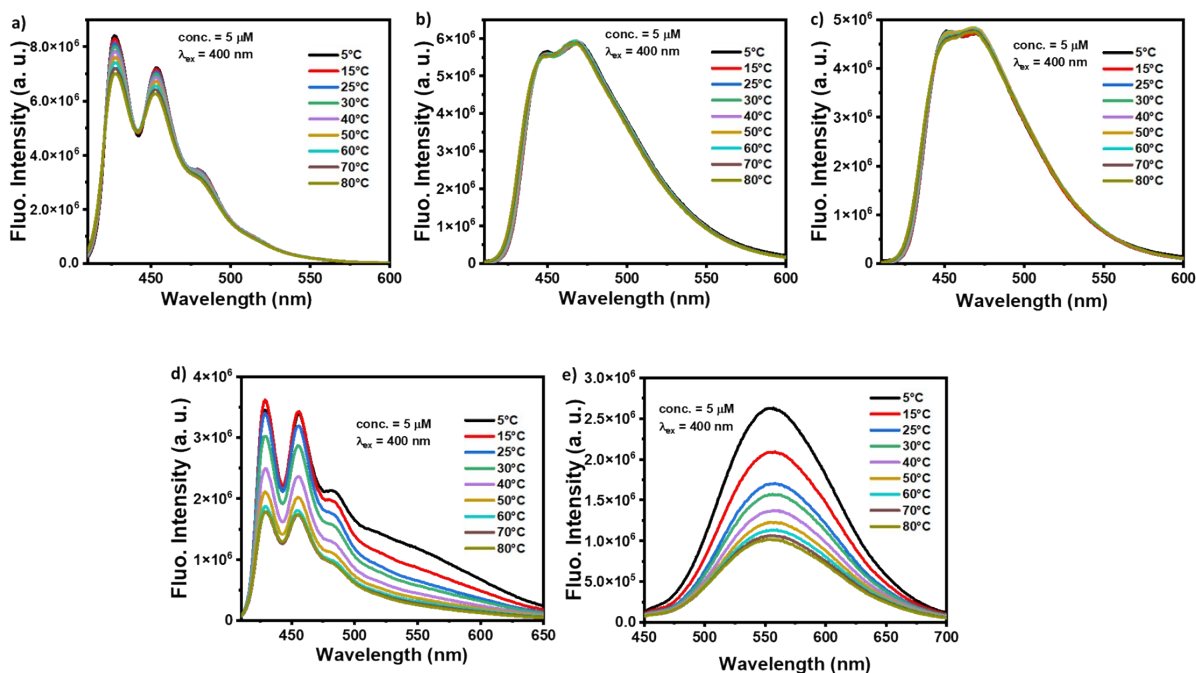


Fig. S14. Temperature-dependence of emission spectra of (a) AnP, (b) AnPCO₂Me, (c) AnPCN, (d) AnPCHO and (e) AnPNMe₂ ($\lambda_{\text{ex}} = 400 \text{ nm}$) ($5 \mu\text{M}$) in Propylene glycol.

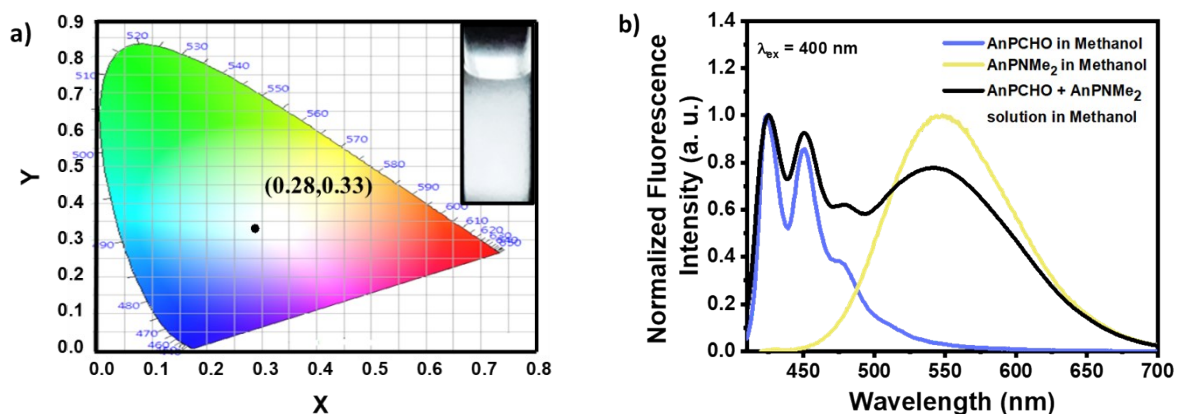


Fig. S15. (a) CIE chromaticity diagram of the WLE solution obtained by mixing methanol solutions of AnPCHO ($5 \mu\text{M}$) and AnPNMe₂ ($5 \mu\text{M}$) in 2:3 ratio (v/v) (inset: luminescence image of the solution under excitation of 400 nm) and (b) normalized emission spectra of AnPCHO, AnPNMe₂ and the WLE solution in methanol ($\lambda_{\text{ex}} = 400 \text{ nm}$).

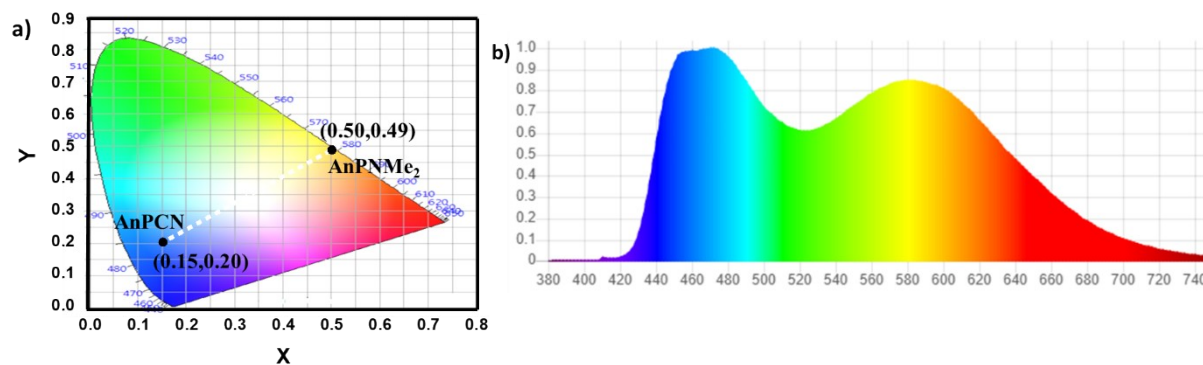


Fig. S16. (a) CIE chromaticity diagram of **AnPCN** and **AnPNMe₂** in DMSO and the connecting line represents the CIE indices of their solutions mixed in different proportions and (b) normalized color spectrum of the emission from the resulting WLE solution by mixing DMSO solutions of **AnPCN** (5 μ M) and **AnPNMe₂** (5 μ M) in 3:22 ratio (v/v).

Table S8. Fluorescence lifetime values of **AnPCN** and **AnPNMe₂** solution in DMSO, WLE solution in DMSO and the WLE gel ($\lambda_{\text{ex}} = 405$ nm).

	$\lambda_{\text{em}} = 456$ nm		$\lambda_{\text{em}} = 588$ nm	
	$\tau(\text{ns})(\beta)(\alpha)$	χ^2	$\tau(\text{ns})(\beta)(\alpha)$	χ^2
AnPCN in DMSO	3.52(100)(100)	1.09	-	-
AnPNMe₂ in DMSO	-	-	3.73(100)(100)	1.14
WLE solution in DMSO	3.52(100)(100)	1.22	3.60(100)(100)	1.29
WLE gel	3.64(100)(100)	1.20	3.12(100)(100)	1.21

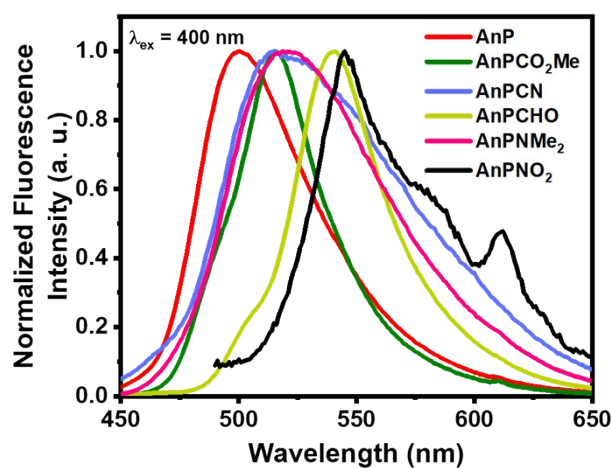


Fig. S17. Emission of the compounds in their solid powder forms.

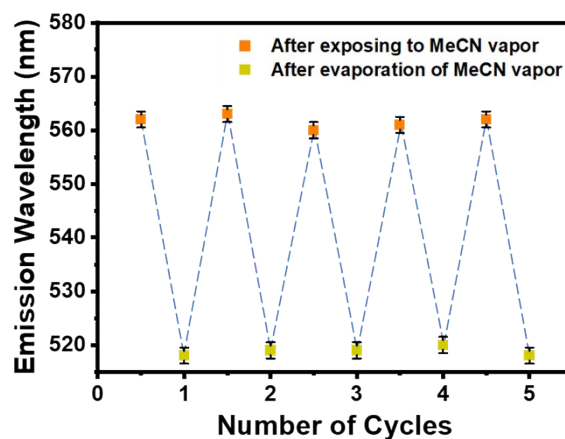


Fig. S18. Plot of emission wavelength vs number of repeated cycles of passing MeCN vapor through TLC plate containing **AnPNMe₂** and evaporating the MeCN vapor (error = ± 2 nm).

- 1 T. Le Bahers, C. Adamo and I. Ciofini, *J. Chem. Theory Comput.*, 2011, **7**, 2498–2506.
- 2 E. von Lippert, *Zeitschrift für Elektrochemie*, 1957, **61**, 962–975.
- 3 J. R. Lakowicz, *Principles of fluorescence spectroscopy*, Springer, 2006.
- 4 H. Hoshino, S. Okada, H. Urakawa and K. Kajiwara, *Polym. Bull.*, 1996, **37**, 237–244.